A domain adaptation methodology for enhancing the classification of structural condition states in continuously monitored historical domes

Received: 4 March 2024 | Accepted: 16 July 2024

DOI: 10.1111/mice.13313

COMPUTER-AIDED CIVIL AND INFRASTRUCTURE ENGINEERING WILEY

RESEARCH ARTICLE

A domain adaptation methodology for enhancing the classification of structural condition states in continuously monitored historical domes

V. Cavanni[1] | **R. Ceravolo**[1,2] | **G. Miraglia**[1,2]

[1]Department of Structural, Geotechnical and Building Engineering, Politecnico di Torino, Turin, Italy

[2]Responsible Risk Resilience Interdepartmental Centre (R3C), Politecnico di Torino, Turin, Italy

Correspondence
R. Ceravolo, Politecnico di Torino, C. Duca degli Abruzzi 24, Turin 10129, Italy.
Email: rosario.ceravolo@polito.it

Funding information
Next Generation EU within the PRIN 2022 PNRR program, Grant/Award Number: D.D.1409 14/09/2022 MIUR

Abstract

The unavailability of labeled data has always been the main limitation of data-driven solutions for monitoring the health state of full-scale structures. In this area, domain adaptation (DA) solutions have occasionally been proposed in recent years, which allow the sharing of data sets between distinct but similar systems. This paper presents a novel computational methodology to evaluate the condition state of historical buildings subjected to continuous monitoring. The DA method, specifically transfer component analysis, is used to maintain correlations between two data domains with low relevance, thereby improving the accuracy of classification models. Additionally, it is shown that the kernelized Bayesian transfer learning can enhance classification accuracy beyond what is achievable with a support vector machine. The paper is completed with a real-world application to the classification of data sets from two Italian Baroque churches, both characterized by imposing oval masonry domes, but equipped with very different monitoring systems.

1 | INTRODUCTION

Recently, artificial intelligence (AI) is proving to be a useful tool in the field of structural health monitoring (SHM) and integrated structural control and health monitoring (ISCHM) (Farrar & Worden, 2012; Javadinasab Hormozabad et al., 2021; Pezeshki, Adeli, et al., 2023), especially machine learning (ML), which is increasingly used to manage data and perform predictions (Adeli & Hung, 1994; Amezquita-Sancheza et al., 2020; Farrar & Worden, 2012; Pavlou, 2022; Perez-Ramirez et al., 2019). ML algorithms are trained on a data set that may or may not be labeled, and then used to perform predictions on new data. The main limits of *supervised algorithms*, that is, algorithms trained for classification with labeled data sets, are the need to provide a minimum of observations for each class considered, which in the examined case are structural condition states, for example, damage or even just temperature (Rafiei & Adeli, 2017). Training data sets consist of several *features*, which can be, for instance, modal parameters, as they reflect variations in structural conditions, be they pathological or physiological. These features are obtained through an identification procedure (Ceravolo et al., 2016; Perez-Ramirez et al., 2016) developed from the signal recorded during dynamic monitoring of the structure and are structurally significant for any kind of existing systems (Pezeshki, Pavlou, et al., 2023). It is therefore possible to understand that in most full-scale structures, it

is difficult or even impossible to find data sets describing all possible structural conditions, as it is not possible to deliberately act on the structure to obtain information on different conditions. The lack of labeled data is a crucial aspect that must be addressed to develop an ML model that can perform well for new unseen data.

In this view, new methods, such as transfer learning (TL), are required to compensate for insufficient labeled data. The problem is addressed by considering data from different systems, which can be different but, in some way, related, and by manipulating them with domain adaptation (DA) techniques (Pan & Yang, 2009). The concept behind TL with DA is to exploit data, that is, knowledge, from "*third-parties systems*" to improve the prediction capability of a classifier for the investigated system about which a little amount of data are available. Therefore, a proper choice of the system(s) from which to retrieve data is essential; indeed, it is likely that the more similar that system(s) is to the one being investigated, the better the information transfer will be. When the investigated system is an observed structure, the exploited system may be a mathematical model of it, such as a calibrated finite element model (FEM) (Ceravolo et al., 2016), or other observed structures that have some correspondence with the investigated one. The set of structures considered generates a population that may be *homogeneous* or *heterogeneous* according to the dissimilarity that exists among them in terms of geometry, material, and topology (Bull et al., 2020; Gardner, Bull, et al., 2020).

The strategy of enriching monitoring data sets by drawing from richer domains is increasingly being applied to engineering structures. References can be made to Huang et al. (2024), Lin et al. (2022), and Quqa et al. (2023) for simulation-to-real information transfer in beams, sheets, and rails; Li et al. (2021) for pavement distress detection; Chakraborty et al. (2011) for the classification of fatigue damage in an aluminum lug joint; and Gao and Mosalam (2018) and Giglioni et al. (2024) for damage detection.

Instead, in this work, a full computational procedure is proposed to transfer knowledge between full-scale structures subjected to continuous monitoring, specifically historical domes. Indeed, monitoring practices play a crucial role in historical buildings (Ceravolo et al., 2016), providing first-hand data for decision making. The continuous observation of the entire structure, as well as the objective and accurate information on the performance and structural integrity that only permanent monitoring can achieve, favors the implementation of preventive conservation and the execution of targeted interventions, containing costs, invasiveness, and risks of irreparable damage.

First, the homogeneous TL between a continuously monitored structure and its FEM is addressed, taking advantage of a preliminary study that used the FE model of the Sanctuary of Vicoforte, which features one of the most monitored historical domes in the world (Coletta et al., 2021). In this case, a DA is realized through a transfer component analysis (TCA) (Pan et al., 2011) and the classification is performed with a relevance vector machine (RVM) model (Tipping, 2001). A heterogeneous perspective of TL is then proposed for which information obtained from the monitoring activities of a structure is transferred to enhance the prediction accuracy of data representative of the less monitored structure. A suitable tool for transferring knowledge between different monitoring systems is kernelized Bayesian transfer learning (KBTL) (Gönen & Margolin, 2014), a supervised algorithm that performs a heterogeneous TL with DA. The experimental verification of the heterogeneous case is conducted on continuous monitoring data sets of two oval domes, respectively, of the Sanctuary of Vicoforte and of the Church of Santa Caterina in Casale Monferrato.

The paper is organized as follows. Section 2 is intended to provide an overview on DA, and specifically on TCA and KBTL. In Section 3, the main types of application of TL for SHM, a brief description of the case studies used to define the methodology and the methodology itself are introduced.

Section 4 illustrates the experimental verification of the methodology proposed for the two historical domes, via the application of TCA and KBTL. In Section 5, conclusions are drawn.

2 | THEORETICAL BACKGROUND

This section initially takes up the definitions and concepts underlying the TL with DA, which is conceptually different from the fine-tuning approaches generally used to exploit existing deep neural networks. Thereafter, in specific subsections, the two algorithms used in the proposed computational procedure are briefly described, with their principal hypotheses and assumptions, to provide an overview and justify their choice. For the description of the approach with TCA, one may refer to the article by Pan et al. (2011), whereas for KBTL method, reference is made to the paper by Gönen and Margolin (2014) and to the paper by Gardner et al. (2022), where the first application of this algorithm to framed laboratory structures was presented.

For simplicity, matrices will be indicated with bolded uppercase characters, vectors with bolded lowercase characters, and scalar variables with italic lowercase characters.

DA is a TL technique applied to induce an improvement in the predictive ability of a model for a given domain that contains insufficient data by exploiting knowledge learned by the model in the training phase from

third-party domains with adequate labeled data. Each domain is composed by an input feature space $\mathcal{X}$ and a marginal probability distribution $P(\mathbf{X})$ of a set $\mathbf{X} = \{\mathbf{x}_1; \ldots; \mathbf{x}_N\} \in \mathcal{X}$, with $\mathbf{x}_i$ the ith observation of the features vector. To each domain, a task $\mathcal{T} = \{\mathcal{Y}; f(\cdot)\}$ is associated, where $\mathcal{Y}$ is the label space and $f(\cdot)$ the objective predictive function, which can also be seen as a conditional distribution $f(x) = P(y|x)$ (Farahani et al., 2020). To develop a DA, two domains are required, specifically the target and the source one. The first, D_t, is the reference domain for which the network is trained, but which contains too few data to obtain accurate predictions and it can be composed of labeled or partially labeled data:

$$D_t = \left\{\mathbf{x}_{t,i}, y_{t,i}\right\}_{i=1}^{N_t} \text{ where } \mathbf{x}_{t,i} \in \mathcal{X}_t \text{ and } y_{t,i} \in \mathcal{Y}_t \tag{1}$$

with i free variable that indicates the ith sample. The second, D_s, in the case of a single-source TL (i.e., only one system is considered as source), is the domain of labeled data that is exploited to increase performance on making prediction of data belonging to the target domain (TD):

$$D_s = \left\{\mathbf{x}_{s,i}, y_{s,i}\right\}_{i=1}^{N_s} \text{ where } \mathbf{x}_{s,i} \in \mathcal{X}_s \text{ and } y_{s,i} \in \mathcal{Y}_s \tag{2}$$

where N_s and N_t are the number of observations in the source domain (SD) and TD, respectively, and generally $0 < N_t \ll N_s$.

Depending on the relation between the feature spaces and label spaces of the two domains, different TL models can be distinguished, specifically a homogeneous or heterogeneous TL can be performed. The first assumes that the feature and the label spaces are shared by the two domains, meaning $\mathcal{X}_t = \mathcal{X}_s$ and $\mathcal{Y}_t = \mathcal{Y}_s$, and therefore the dimensions of the feature spaces are equal, that is, $d_s = d_t$. Unlike, the second assumes that the feature spaces are not equivalent, that is, $\mathcal{X}_t \neq \mathcal{X}_s$, and often that the SD and TD do not have the same feature space dimension, that is, $d_s \neq d_t$; additionally, it can also assume different label spaces, $\mathcal{Y}_t \neq \mathcal{Y}_s$ (Farahani et al., 2020). Regardless of the type of TL to be developed (homogeneous or heterogeneous), the two domains will differ in the marginal distributions, that is, $P(\mathbf{X_s}) \neq P(\mathbf{X_t})$. DA approaches are therefore involved with the aim of reducing the distance between these marginal distributions. Furthermore, in the case of different feature space dimensions, the DA is also responsible for the dimensionality reduction (or expansion) of the original domains to the common dimension, $\mathcal{R}$.

2.1 | Transfer component analysis

The TCA is a homogenous TL algorithm introduced by Pan et al. (2011) that via DA tries to preserve as much as possible the data variance, and to reduce the distance between different distributions across domains, in order to enable the transfer of knowledge between distinct domains. This is performed with a dimensionality reduction in a reproducing kernel Hilbert space (RKHS), spanned by the learned components, employing the maximum mean discrepancy (MMD) criterion.

TCA assumes that $P(\mathbf{X_s}) \neq P(\mathbf{X_t})$ and $P(\mathbf{Y_s}|\mathbf{X_s}) = P(\mathbf{Y_t}|\mathbf{X_t})$, requiring that $\mathcal{X}_t = \mathcal{X}_s$ and $\mathcal{Y}_t = \mathcal{Y}_s$ correspond to a homogenous TL approach. The MMD distance between the empirical means of the two domains, $Dist(\mathbf{X}'_\mathbf{s}, \mathbf{X}'_\mathbf{t})$, reads:

$$Dist\left(\mathbf{X}'_\mathbf{s}, \mathbf{X}'_\mathbf{t}\right) = tr\left(\mathbf{KL}\right) \tag{3}$$

where $\mathbf{X}'_\mathbf{s}$ and $\mathbf{X}'_\mathbf{t}$ are the inputs transformed form of the SD and TD, $\mathbf{K} \in \mathbb{R}^{(N_s+N_t)\times(N_s+N_t)}$ is a kernel symmetric matrix, containing the kernel matrices of source, target, and cross domains, and $\mathbf{L}$ is the MMD matrix.

The kernel matrix can be decomposed as $\mathbf{K} = (\mathbf{K}\mathbf{K}^{-0.5})\ (\mathbf{K}^{-0.5}\mathbf{K})$, defined as the empirical kernel map. By exploiting a matrix $\tilde{W} \in \mathbb{R}^{(N_s+N_t)\times m}$, the empirical kernel map features are transformed into an m-dimensional space (with $m \ll N_s + N_t$ hyperparameter to be selected) obtaining the resultant kernel matrix as:

$$\tilde{\mathbf{K}} = \left(\mathbf{K}\mathbf{K}^{-0.5}\tilde{\mathbf{W}}\right)\ \left(\tilde{\mathbf{W}}^\intercal\mathbf{K}^{-0.5}\mathbf{K}\right) = \mathbf{K}\mathbf{W}\mathbf{W}^\intercal\mathbf{K} \tag{4}$$

with the transformation matrix $\mathbf{W} = \mathbf{K}^{-0.5}\ \tilde{\mathbf{W}}$.

To minimize the MMD distance, a regularization term is needed to control the complexity of the matrix $\mathbf{W}$, hence the kernel learning problem becomes:

$$\min_{\mathbf{W}} tr\left(\mathbf{W}^\intercal\mathbf{K}\mathbf{L}\mathbf{K}\mathbf{W}\right) + \mu\, tr\left(\mathbf{W}^\intercal\mathbf{W}\right) \quad \text{s.t. } \mathbf{W}^\intercal\mathbf{K}\mathbf{H}\mathbf{K}\mathbf{W} = \mathbf{I} \tag{5}$$

where the second term is the product between a trade-off parameter ($\mu > 0$) and the regularization term ($tr(\mathbf{W}^\intercal\mathbf{W})$), $\mathbf{H}$ is a centering matrix, $\mathbf{I} \in \mathbb{R}^{m\times m}$ is an identity matrix, and the constraint $\mathbf{W}^\intercal\mathbf{K}\mathbf{H}\mathbf{K}\mathbf{W} = \mathbf{I}$ is introduced to avoid the trivial solution $\mathbf{W} = 0$.

Then, Equation (5) can be solved with the equivalent trace optimization problem:

$$\max_{\mathbf{W}} tr\left(\left(\mathbf{W}^\intercal\left(\mathbf{K}\mathbf{L}\mathbf{K} + \mu\mathbf{I}\right)\mathbf{W}\right)^{-1}\mathbf{W}^\intercal\mathbf{K}\mathbf{H}\mathbf{K}\mathbf{W}\right) \tag{6}$$

as can be seen from the Lagrangian of Equation (5). The solutions for $\mathbf{W}$ in Equation (6) are the m leading eigenvectors of $(\mathbf{K}\mathbf{L}\mathbf{K} + \mu\mathbf{I})^{-1}\mathbf{K}\mathbf{H}\mathbf{K}$, where $m \leq N_s + N_t - 1$, which are used to define the space of the transformed features through $\mathbf{Z} = \mathbf{K}\mathbf{W}$, where $\mathbf{Z} \in \mathbb{R}^{(N_s+N_t)\times m}$.

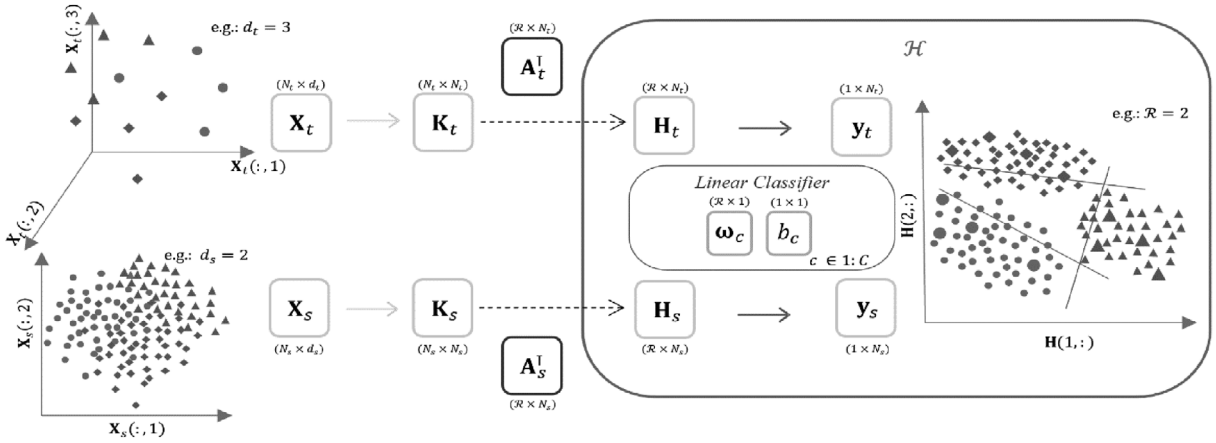

FIGURE 1 Overview on kernelized Bayesian transfer learning (KBTL) conceptual flow for a target domain t and a source domain s. Graphical representations are also presented of the original domains, target (e.g., $d_t = 3$) and source (e.g., $d_s = 2$), with a common label space of three classes (multiclass problem), and of the same domains projected in the latent subspace $\mathcal{H}$ with the linear classifier for each class (*one-versus-all*).

2.2 | Kernelized Bayesian transfer learning

The KBTL is a heterogeneous supervised learning algorithm used to share knowledge within a population and admits the features inconsistency. This model has been introduced by Gönen and Margolin (2014) to share knowledge across multiple data sets from different systems generating a linear classification model in a shared latent subspace.

This model assumes T domains $\{D_k\}_{k=1}^{T}$ with inconsistent feature spaces $\{\mathcal{X}_k\}_{k=1}^{T}$. Each domain has an associated task $\{\mathcal{T}_k\}_{k=1}^{T}$ with consistent label spaces $\mathcal{Y}_j = \mathcal{Y}_r \; \forall \; j, r \in 1{:}T$, hence a global and unique label space $\mathcal{Y}$ shared among the T domains can be assumed. Each kth domain has N_k finite feature observations $\mathbf{X}_k = \{\mathbf{x}_{k,i} \in \mathcal{X}_k\}_{i=1}^{N_k}$ at which correspond a finite set of N_k label observations $\mathbf{y}_k \in \mathcal{Y}$. The label space $\mathcal{Y}$ is composed by C classes (i.e., $C = 2$ for binary problem, $C > 2$ for multiclass problem). For each kth domain/task pair, there is a specific kernel function $k_k(\cdot, \cdot)$ that defines the correlation between the observations of the kth domain and therefore each domain is represented by its own kernel matrix $\mathbf{K}_k = k_k(\mathbf{X}_k, \mathbf{X}_k')$.

Conceptually, the algorithm can be summarized in two main phases: projection of data points from the different domains into a shared latent subspace $\mathcal{H}$, using a kernel-based dimensionality reduction model for each domain, and deduction of a linear discriminative classifier in the shared latent subspace (see Figure 1). The first phase has been designed to manage the inconsistent feature spaces and to reduce the distance between the distributions. Indeed, considering two domains D_j and D_r with dimensions d_j and d_r, with $d_j \neq d_r$, if a classifier within these domains has to be obtained, both domains have to be projected into a shared latent subspace through a dimensionality reduction to the dimension $\mathcal{R}$ of the latent subspace $\mathcal{H}$. To perform it, each domain k has to be represented with its own kernel matrix $\{\mathbf{K}_k \in \mathbb{R}^{N_k \times N_k}\}_{k=1}^{T}$ and the representation of the datapoints in the shared latent subspace $\mathcal{H}$ is subsequently obtained by premultiplying the kernel matrix for the transpose of the optimal linear projection matrix $\{\mathbf{A}_k \in \mathbb{R}^{N_k \times \mathcal{R}}\}_{k=1}^{T}$, learned by the algorithm. The final representation of each domain in the shared latent subspace is described as $\{\mathbf{H}_k = \mathbf{A}_k^{\intercal}\mathbf{K}_k \in \mathbb{R}^{\mathcal{R} \times N_k}\}_{k=1}^{T}$. The KBTL can be used for binary classification or multiclass classification, which corresponds to the model used in this paper. Consequently, only the hypotheses for this second case are reported, while for additional details one can refer to Gönen and Margolin (2014). The second stage is the classification part that calculates the predicted outputs in the shared latent subspace $\mathcal{H}$. This is performed for a multiclass problem with a linear classifier for each class c, $\mathbf{f}_{k,c} = \mathbf{H}_k^{\intercal}\boldsymbol{\omega}_c + \mathbf{1}b_c \; \forall \; k \in 1:T$ and $\forall \; c \in 1:C$, where the weights vector $\{\boldsymbol{\omega}_c \in \mathbb{R}^{\mathcal{R} \times 1}\}_{c=1}^{C}$ and the bias $\{b_c \in \mathbb{R}^{1 \times 1}\}_{c=1}^{C}$ are the classifier parameters learned by the algorithm for each class and shared among all the domains.

In Figure 2, a graphical representation of the KBTL model for multiclass classification is reported, where it is possible to identify all the priors, the hyperparameters, and the latent variables. In detail, three priors are present, namely, the matrix of priors $\{\boldsymbol{\Lambda}_k \in \mathbb{R}^{N_k \times \mathcal{R}}\}$ of the task-specific projection matrix $\mathbf{A}_k$, the vector of priors $\{\boldsymbol{\eta}_c \in \mathbb{R}^{\mathcal{R} \times 1}\}$ of the weights vector $\boldsymbol{\omega}_c$, and the prior $\{\gamma_c \in \mathbb{R}^{1 \times 1}\}$ for the bias parameter b_c. Each of these three priors is defined from a set of two hyperparameters $\{\alpha_\lambda, \beta_\lambda\}$ for $\boldsymbol{\Lambda}_k$, $\{\alpha_\eta, \beta_\eta\}$ for $\boldsymbol{\eta}_c$ and $\{\alpha_\gamma, \beta_\gamma\}$ for γ_c. The variance of the shared latent subspace is introduced as σ_h^2. Since it is a multiclass classification model, each class has its own set

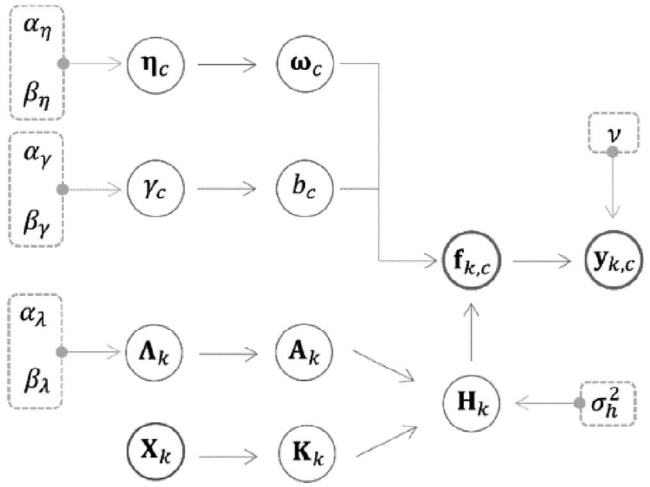

FIGURE 2 Graphical representation of kernelized Bayesian transfer learning (KBTL) model for multiclass classification, with hyperparameters (dashed), input data set ($\mathbf{X}_k$), parameters for the dimensionality reduction and projection in the latent subspace, and classifier parameters.

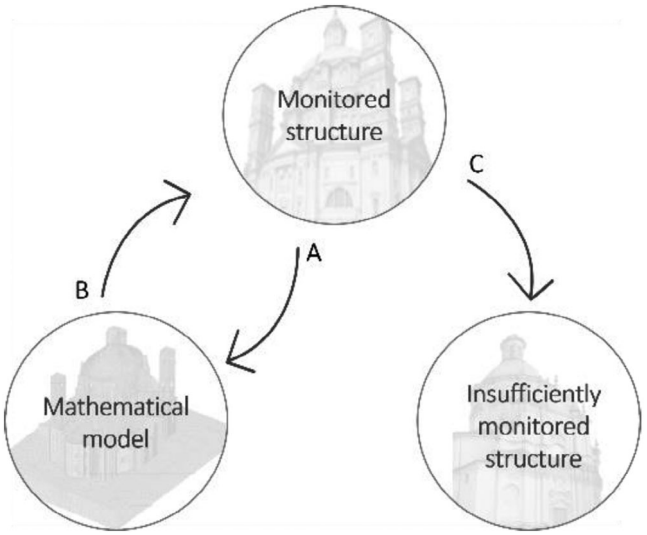

FIGURE 3 Different source–target combinations for application of transfer learning (TL) to structural health monitoring (SHM). (a) TL from the experimental data sets of a monitored structure to the simulated ones; (b) TL from the simulated data sets of a monitored structure to the experimental ones; (c) TL from the experimental data sets of a monitored structure to the experimental data sets of an insufficiently monitored one.

of classifier parameters $\{b_c \in \mathbb{R}^{1\times1}, \omega_c \in \mathbb{R}^{\mathcal{R}\times1}\}$, which are shared by the domains. Indeed, the model is built in a *one-versus-all* manner, which means that each class has its own classifier that separates it from the other classes. This implies that for each class, the probability that a given datapoint is a subset of it is computed, then the label assigned to the datapoint will be the one for which the highest probability has been computed. Several assumptions are used for the distributions: (i) Normal distribution, $\mathcal{N}(\cdot;\boldsymbol{\mu},\boldsymbol{\Sigma})$, for $\mathbf{A}_k(i,s)|\boldsymbol{\Lambda}_k(i,s)$; $\mathbf{H}_k(s,i)|\mathbf{A}_k(:,s),\mathbf{K}_k(:,i)$; $b_c|\gamma_c$; $\omega_c(s)|\eta_c(s)$ and $\mathbf{f}_{k,c}(i)|b_c,\omega_c$, $\mathbf{H}_k(:,i)$; (ii) Gamma distribution, $\mathcal{G}(\cdot;\alpha,\beta)$, for $\boldsymbol{\Lambda}_k(i,s)$; γ_c and η_c; and (iii) Kronecker delta function $\mathbf{y}_{k,c}(i)|\mathbf{f}_{k,c}(i) \sim \delta(\mathbf{f}_{k,c}(i)\mathbf{y}_{k,c}(i) > \nu)$; where, $k \in 1:T$, $i \in 1:N_k$, $s \in 1:\mathcal{R}$ and ν is the nonnegative margin parameter, introduced to find a low-density region among the classes (closely to the idea of a support vector machine model).

To realize an efficient inference mechanism, Gönen and Margolin (2014) developed a variational method that uses a lower bound on the marginal likelihood using an ensemble of factored posteriors to find the joint parameter distribution. To bound the marginal likelihood, the Jensen's inequality is exploited, and it is optimized by maximizing it with respect to each factor until convergence, for more details about this, the authors suggest referring directly to Gönen and Margolin (2014).

The approximate posterior distributions for the multiclass problem result with the same distribution as the corresponding factors. The predictive equations for the projection and dimensionality reduction part, the predictive distribution of the predicted output, and the predictive distribution of the class label are written by substituting the true posteriors with the approximate posterior distributions (Gönen & Margolin, 2014).

3 | APPLICATION TO EVALUATING THE CONDITION OF HISTORICAL DOMES: EXAMPLE MODELS AND PROPOSED METHODOLOGY

TL has various potential uses in monitoring full-scale structures, depending on the domains (source and target) chosen. The substantial difference lies above all in the "*nature*" of the data to be exploited; specifically, it is possible to work with experimental data (i.e., obtained directly from sensors placed on the structure) or with data obtained by model simulations, such as FEMs. From these two types of data sets, which will henceforth be referred to as *experimental data set* (from monitoring) and *simulated data set* (from the model), it is possible to obtain three possible source–target combinations (Figure 3).

Figure 3a: TL from experimental data set to simulated data set. The purpose of this type of application of TL is to calibrate the mathematical model (e.g., FEM) of a structure, thereby obtaining a *digital twin* that can later be exploited as a means of simulating any structural condition, thus predicting the response of the real structure. Nevertheless, to perform a model calibration, a quite extensive monitoring campaign is required, consequently only for highly monitored structures is there a real possibility

of creating a predictive model. Currently, model updating procedures are successfully performed without the need to resort to TL techniques (e.g., Friswell & Mottershead, 1995). This derives from the great availability of linear FEM formulations and the high level of accuracy achieved by the local and global sensitivity methods proposed in the literature (e.g., Boscato et al., 2015; Bursi* et al., 2014; Ceravolo et al., 2020). The application of TL, specifically DA techniques, could in the future make the process faster and therefore more convenient for matching nonlinear and complex behaviors. In cases where it was possible to reach a level of correspondence for which the two domains were almost overlapping, one could, in perspective, consider each characteristic simulated on the model in the same way as data extrapolated directly from the monitored structure. This would lead to overcoming one of the fundamental limitations of using ML in SHM, namely, the difficulty in finding data from damaged conditions to train supervised algorithms.

Figure 3b: TL from simulated data set to experimental data set. When an accurate (e.g., experimentally calibrated) model of the structure is available, this can be exploited to simulate those structural conditions for which few data from direct monitoring of the structure are available. Since, however, in most of the cases, the experimental data set and the simulated data set are not perfectly overlapped, a TL with DA can be implemented in order to reduce the distance between the two data distributions by allowing a classification (or regression) model to be generated in a latent space shared by the two domains, thus compensating the limitations of experiments with simulations.

Figure 3c: TL from an experimental data set to another experimental data set. Further possible applications occur when data are available from exhaustively monitored structures (e.g., permanent dynamic monitoring system), which can be traced back from a structural point of view to an insufficiently monitored structure (e.g., nonpermanent monitoring, incomplete data sets, periodic or *una tantum* condition assessment tests). In this circumstance, the data of the most monitored structure can be exploited via DA to implement the knowledge of the less monitored structure thus allowing the interpretation of its new data.

Recently, DA has been applied, in varied ways, to simple structural schemes, such as laboratory frames and beams (e.g., Gardner et al., 2022; Gardner, Liu, et al., 2020; Wang & Xia, 2022). The common application of DA is indeed to transfer knowledge from more than one system, that is, consider a TD and different SDs (both from real structures and from models, more or less similar to the target structure). Another possible point of view presented in literature is that of sharing knowledge among multiple structures, in which case, the strict meaning of SD and TD would be lost, because each domain would be source and target at the same time. This last approach, in fact, aims at improving the predictive capacity of the model for each structure considered and not just one.

This paper aims to develop the concepts (b) and (c) and materialize them in a full knowledge transfer procedure between data sets of full-scale structures, even very complex ones but with similarities, subject to continuous monitoring.

3.1 | Application models and data sets

This subsection is devoted to the description of the two case studies with the associated dynamic monitoring data sets, from which the *features* of the TL applications have been extracted. The *Sanctuary of Vicoforte* (Figure 4a) and the *Church of Santa Caterina in Casale Monferrato* (Figure 4g) are two well-known Baroque churches, both subjected to a continuous monitoring and characterized by high geometric complexity, as well as uncertainties regarding materials and construction techniques. Except for the similarity in the oval shape of the dome, the two structures present significant differences, both in plan and elevation, which leads to the development of substantially different dynamic responses. For this reason, it is believed that the two churches form a heterogeneous population (Gardner, Bull, et al., 2020).

The Sanctuary of Vicoforte (Figure 4a) is a baroque monumental building located in Vicoforte (Cuneo, Italy) and famous for having the world's largest oval masonry dome. The Sanctuary was commissioned in 1596 by Carlo Emanuele I di Savoia to Ascanio Vitozzi, but the construction of the drum–dome system (from 1728 to 1732) is to be attributed to Francesco Gallo with the support of Filippo Juvarra. The oval dome (Figure 4b,d) has a major axis of 37.15 m and a minor axis of 24.80 m.

The plan follows the oval shape of the dome, with a total of five chapels and a main atrium distributed along the perimeter. The dome–drum system has suffered over the years from significant structural problems, partly due to progressive settlements, and, to a large extent, arising from the bold structural configuration of the dome–drum system itself, see Figure 4c. In 1983, concerns over the severe settlement and cracking phenomena affecting the structure prompted the decision to put in place a strengthening system (1985–1987).

It consisted of 56 active steel tie-bars placed within holes drilled in the masonry at the top of the drum along 14 tangents around the perimeter, slightly tensioned by jacks. A static monitoring system was set up to measure strains and stresses in the structure and crack propagation, as well as stresses in the reinforcing tie-bars (re-tensioned in 1997).

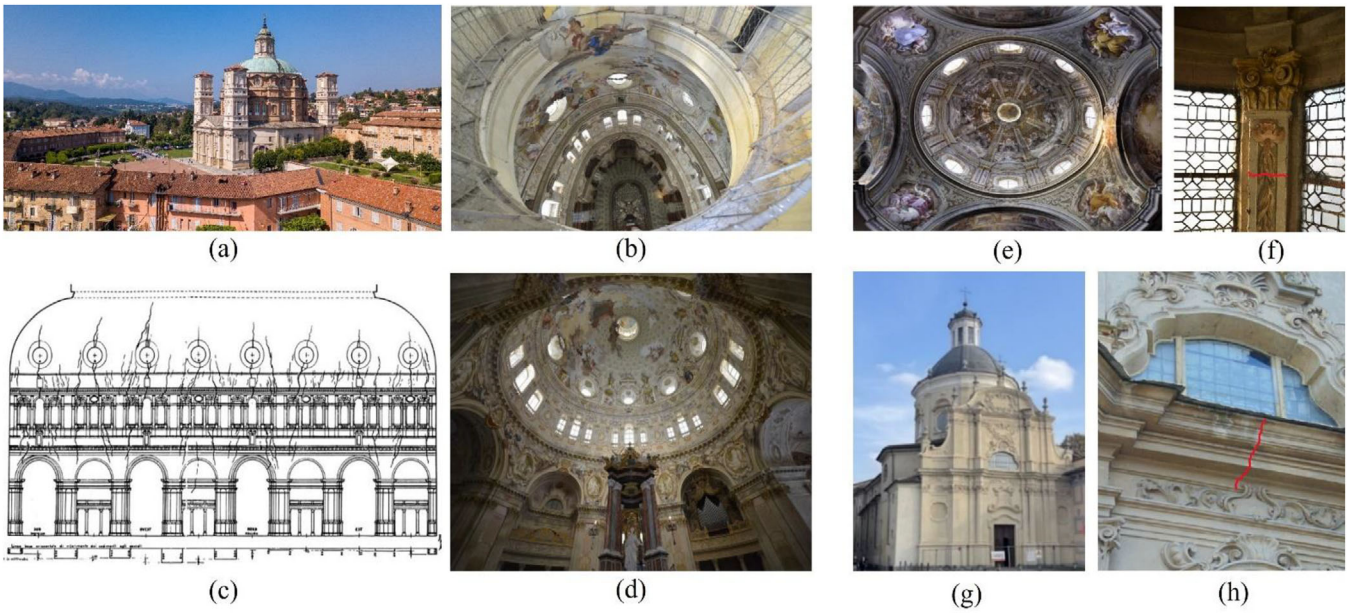

FIGURE 4 Sanctuary of Vicoforte: (a) external view (Pixelshop - stock.adobe.com), (b) internal view from the lantern, (c) crack pattern of the dome (Garro, 1962), and (d) internal view of the dome. Church of Santa Caterina: (e) internal view of the dome, (f) horizontal crack on a pillar of the lantern, (g) external view, and (h) façade vertical crack. All the crack patterns are those observed before the strengthening interventions.

Static monitoring data sets will not be used in this study; however, their analysis was the subject of recent in-depth research to which the reader may refer Ceravolo et al. (2017, 2021). The permanent dynamic monitoring system (Pecorelli et al., 2020) of the lantern–drum–dome system was installed in December 2016 and consisted of 12 monoaxial piezoelectric accelerometers (PCB Piezotronic, model 393B12). Three orthogonal accelerometers were located in the crypt base to record the ground accelerations, while the others were placed at different height of the lantern–drum–dome element, specifically two sensors at the base of the dome, three sensors on the dome, and one vertical accelerometer at the base of the lantern. The system acquires data from the accelerometers as response to ambient vibrations; those of the crypt are first transmitted to a slave unit and then to the master unit, while all other data are directly stored in the master unit. Thereafter, the data are continuously transmitted to the Earthquake Engineering and Dynamics lab (EED lab) of the Politecnico di Torino. The system was set to record data for 20 min every hour, and additionally when the ground horizontal accelerations exceeds a preset threshold value (0.03 g). The Sanctuary is provided with an automatic output-only identification procedure (Pecorelli et al., 2020), based on stochastic subspace identification (SSI) and clustering techniques, to estimate the main modal vibration parameters. The natural frequencies identified are represented in Figure 5a,b, as a function of the days of recording and the environmental temperature, respectively.

The Church of Santa Caterina (Figure 4g), located in Casale Monferrato (Alessandria, Italy), is considered a masterpiece of baroque architecture with a Greek cross plan and characterized by a prominent oval masonry dome (Figure 4e) with a major axis of 14 m, a minor axis of 10 m, and a height of about 4.5 m. In 1718, the construction of the new church began, starting from *Palazzo Marchionale* previously donated to the Dominican nuns. The church consists of two halls: the inner one known as the nuns' choir (10×22 m), a private prayer place for the nuns, and the outer one, open to the public, directly faces Piazza Castello with the main façade of approximately 19 m of height, which juts out from the church body of about 6 m. The central room of the external church supports the oval dome set on the drum (7 m high), with eight large columns. The dome is characterized by eight ribs and is topped by a 6-m-tall lantern.

In 2010, an extensive dynamic campaign has been carried out that highlighted a significant degradation of the lantern (Figure 4f), the drum–dome system and the façade (Figure 4h), caused by water infiltrations (Ceravolo et al., 2016). Consequently, two strengthening interventions have been implemented to increase the stiffness of the lantern and of the façade. Specifically, for the lantern, a system of structural steel composed of 16 L-shaped profiles, positioned along the columns in correspondence of the internal corner of the windows, and of three C-shaped profiles, placed on the window openings, has been installed to promote a global behavior. While for the façade, a metal frame,

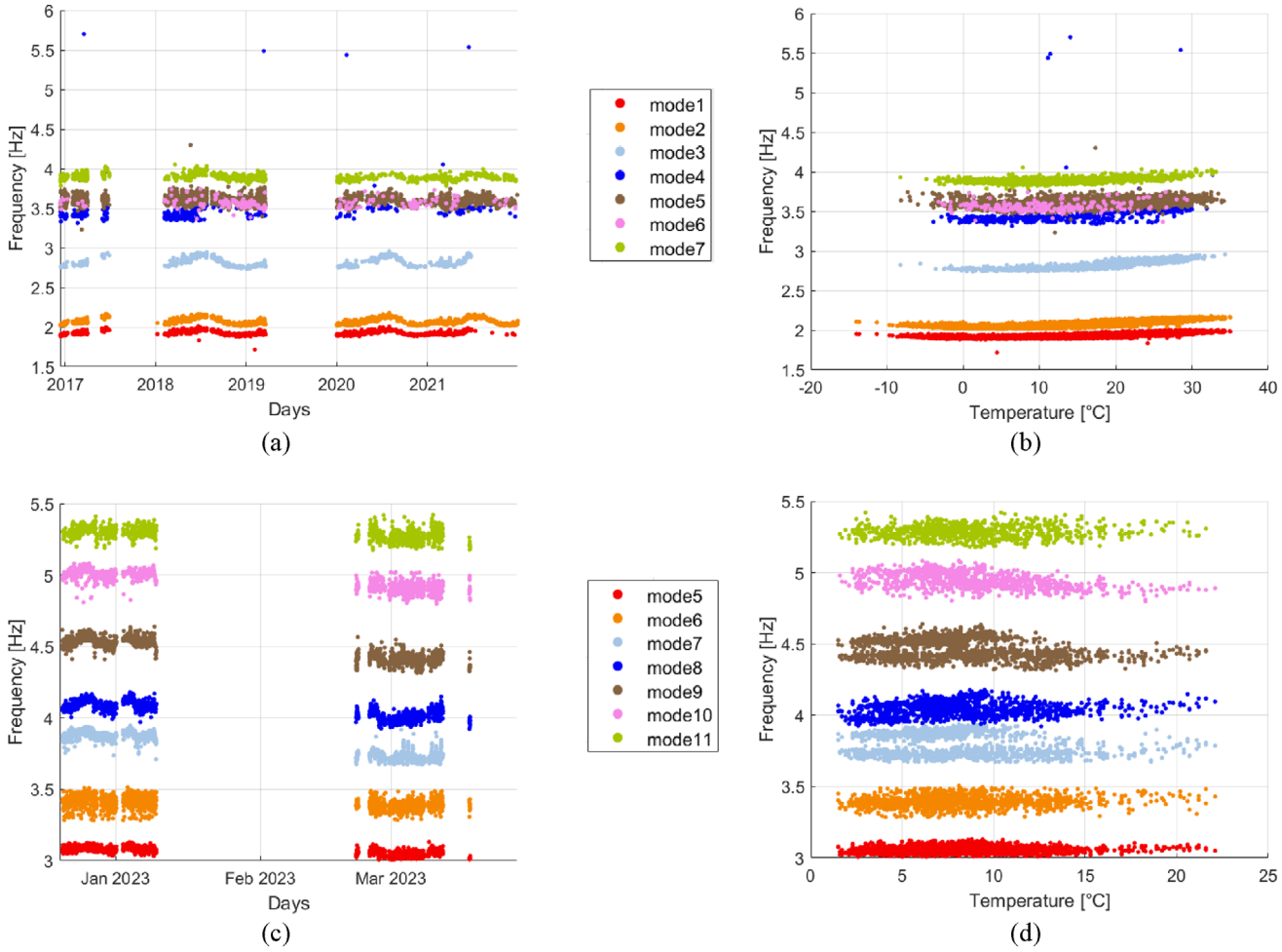

FIGURE 5 Daily time series of the natural frequencies of the Sanctuary of Vicoforte (a) and its frequency–temperature law (b); daily time series of the natural frequencies of the Church of Santa Caterina (c) and its frequency-temperature law (d).

composed by chains, inclined props, and vertical uprights, has been connected to the inner part of to the tympanum (cantilever portion of the façade), to improve the compressive strength of the masonry, by exploiting its greater tensile strength. A description of the damage state before the strengthening interventions can be found in Ceravolo et al. (2024).

From December 2022 to March 2023, the dynamic response of the church to environmental vibrations was recorded with a sparse permanent sensing system, with the aims of collecting and emphasizing the oscillation of modal parameters, notably the natural frequencies of the main modes. These tests were also used as trial field for the design of a permanent dynamic monitoring system, to monitor and control the critical building elements. The setups consists of three accelerometers located on the top of the lantern and positioned to capture the lateral and torsional vibrations of this element. Specifically, two accelerometers were installed to record the accelerations in the transverse directions and one to acquire the longitudinal accelerations, with a sampling frequency for the acquisition of 100 Hz. From a technical perspective, the type of sensors is the same as used at the Sanctuary of Vicoforte, with the difference that here the analog signals are conveyed via three-channel to a Dewesoft® acquisitor (i.e., KRYPTON-4XACC, four channels single ended Krypton slice for Voltage, IEPE) that performs signal conditioning, synchronization, and signal translation from analog to digital format. After data translation, the records in digital format are sent to a computer, which saves data in continuous packets of 10 min, through a 10-m-long data cable. These data packets are automatically stored on a computer located in the EED lab of the Politecnico di Torino, where an identification procedure detects mode 5, mode 6, mode 7, mode 8, mode 9, mode 10, and mode 11. Lower frequency modes, associated with non-structural elements (scaffolding), are discarded. Figure 5c reports the identified natural frequencies as a function of the registration days, while Figure 5d depicts the natural frequencies as a function of temperature.

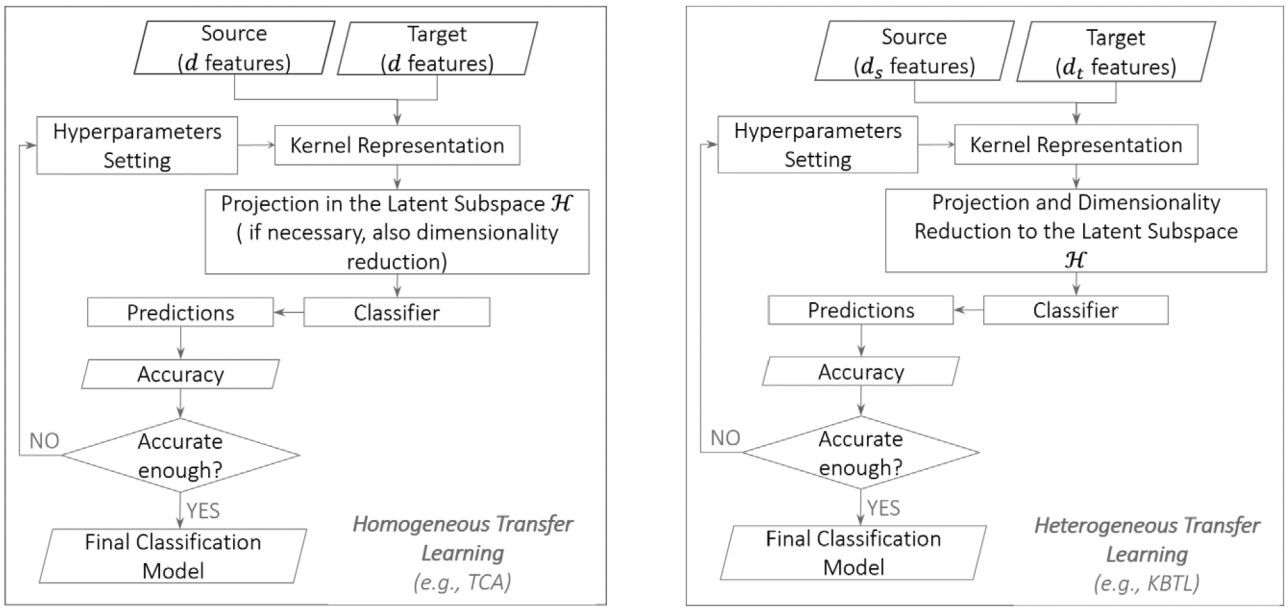

FIGURE 6 Blocks of (a) homogeneous transfer learning (TL) and (b) heterogeneous TL.

3.2 | Outline of the methodology

This subsection presents the outline for a methodology to transfer knowledge between different monitoring systems and models, in order to support diagnosis and decision making for historical domes and buildings. In detail, a flow chart is presented that addresses two types of application of TL to SHM, among those shown in Figure 3, namely, (b) TL from the simulated data sets of a monitored structure to the experimental ones; (c) TL from the experimental data sets of a monitored structure to the experimental data sets of an insufficiently monitored one.

The final goal of the procedure is to track vibration mode fluctuations in time induced by variables that can affect the structural behavior (e.g., environmental and operational variations [EOVs], damage) for both the monitored and the insufficiently monitored structure.

The three main blocks of the procedure are: (a) homogenous TL (Figure 6a), (b) heterogeneous TL (Figure 6b), and (c) model calibration. For the general operation of TL algorithms, specifically DA, refer to Section 2. While the model calibration is developed starting from the experimental measures of the monitored structure and through the definition of the objective function and the stopping criteria. When the updated model is available, the simulations needed are performed.

The three main blocks are linked, as highlighted in the outline of the computational methodology of Figure 7, with two main conceptual branches that lead to track vibration mode fluctuations for the target structure:

1. The selected diagnostic features from the experimental measures, **X1t** (target), and the features simulated after the model calibration, **X0s**, define the input for the development of a homogenous TL (refer to Section 4.1).
2. The selected features of the insufficiently monitored structure, **X2t** (target), and those of a similar monitored one, **X1s**, define the input for the development of a heterogeneous TL (refer to Section 4.2).

It is worth highlighting that the selection of the target features affects the selection of the source features, since only the most relevant ones should be provided to the algorithm.

The paper focuses on the two branches of the methodology involving TL applications, for the experimental verification of which permanent monitoring data sets of two masonry oval domes are used. As for model calibration of historical buildings, one may instead refer to the vast literature on model updating (e.g., Ceravolo et al., 2020).

4 | EXPERIMENTAL VERIFICATION

In this section, the applicability of the above procedure is verified for two Italian Baroque Churches. Given the complexity of the two structures, the application and effectiveness of knowledge transfer between the two is not obvious because of the substantial differences between their dynamic responses. Therefore, this experimental verification aims to test whether the two monitoring systems

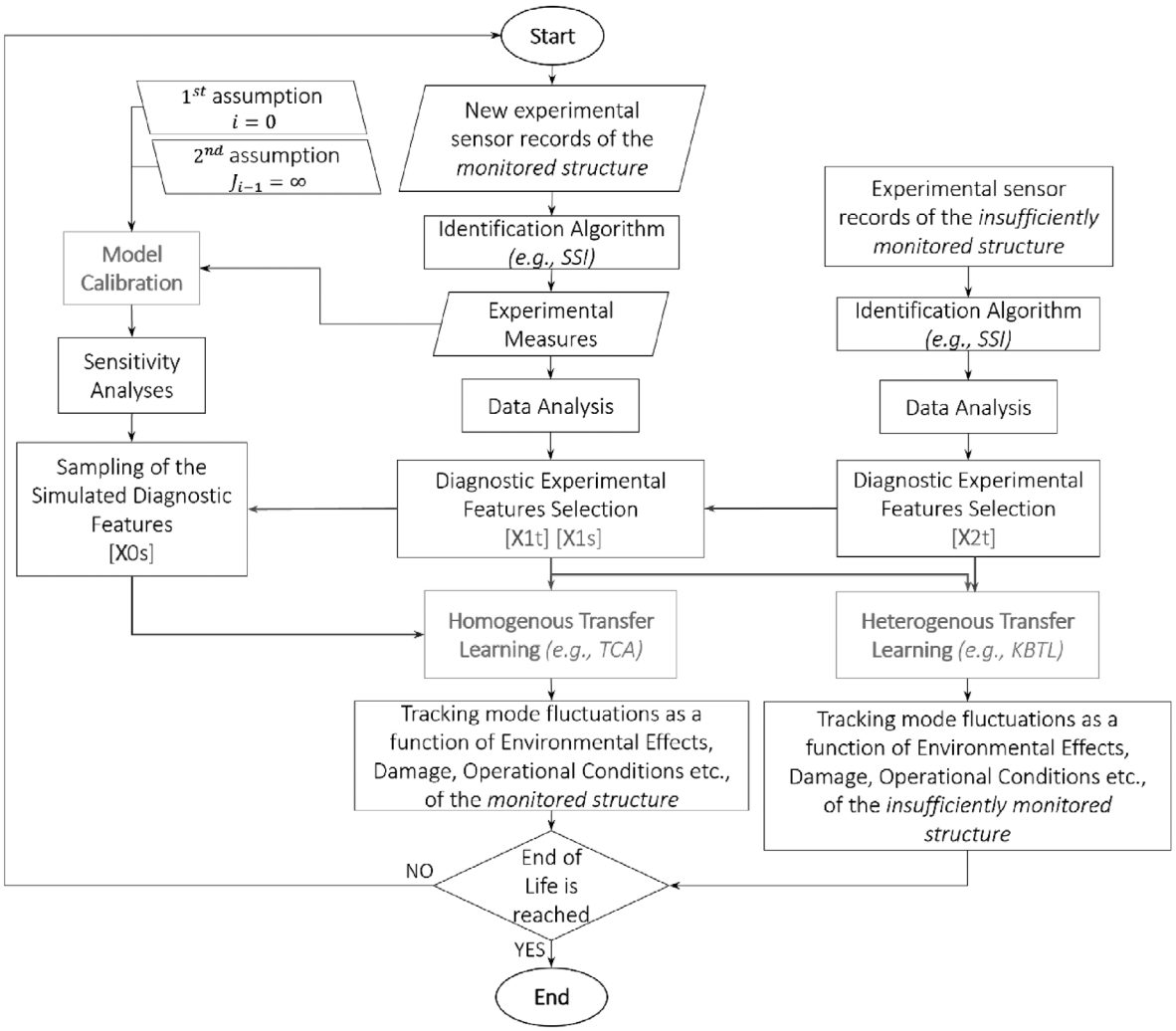

FIGURE 7 Outline of the computational methodology.

and the mathematical model can be brought into communication through the procedure defined above. For this purpose, the classification of temperature states is placed as the ultimate output of the procedure, as a simple demonstration case. Indeed, in order to test a classifier, a reasonable amount of labeled data are needed. While no progression of damage is currently observed in the structures, even as a result of effective cerclage interventions as for Vicoforte dome, the only labeled monitoring data available in large quantities are variations of natural frequencies as a function of temperature. Consequently, also the temperature classes were chosen to obtain as much data as possible for each class for the testing phase, namely, 3°C and 10°C for the homogenous TL and [1.5°C, 3.5°C], [8.5°C, 9.5°C], and [15°C, 18°C] for the heterogeneous one. These classification models also work for different temperature classes, as long as those classes are not adjacent along the temperature axis.

To obtain a numerical evaluation of the efficiency of transfer of knowledge, the results obtained through the two branches of the proposed methodology are compared to simple ML models inferred from the respective TD.

4.1 | TL from simulated data set to experimental data set

TL can be used to integrate experimental data sets that are not able to cover all possible structural conditions, using the FEM simulations of the monitored structure as the SD. To demonstrate this approach, reference is made to the described monitoring data sets of the Vicoforte Sanctuary and to a simple application that contemplates only two temperature classes, specifically 3°C and 10°C (Coletta et al., 2021).

The TD has been associated with the first three natural frequencies of the Sanctuary related to the temperatures 10°C and 3°C. Respectively, 32 and 69 observations are used for the class 1 and class 2. The SD consists of the first three natural frequencies, corresponding to the first two bending

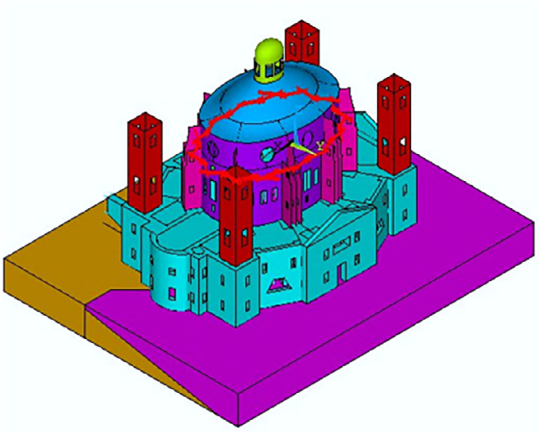

Macro-components	E [GPa]	υ [-]	ρ [Kg/m³]
Bell-towers	4.50	0.35	1800
Basement	2.00	0.35	1800
Buttresses	5.50	0.30	1700
Clay	0.75	0.35	1900
Dome	5.50	0.35	1800
Drum	2.30	0.35	1700
Lantern	5.60	0.35	1800
Marlstone	5.60	0.35	2100
Tie-bars	210	0.30	7800

FIGURE 8 Finite element model (FEM) of the Sanctuary of Vicoforte with the Young's modulus E, Poisson ratio υ, and density ρ values of the nine macrocomponents.

modes in the y and x directions and the torsional mode, obtained through simulations on the numerical model of the Sanctuary. The model is a multiphysics FEM calibrated to reflect the dynamic response of the real structure under ambient noise. Masonry macrocomponents are therefore homogenized into as many linear materials, capable to replicate the experimental vibration modes, both in frequencies (error <1% for first three frequencies) and modal shapes (Ceravolo et al., 2020). It is composed of 119'192 nodes and 210'228 finite elements that contemplate the presence of spring, link, beam, shell, and brick element types. The main structure has been divided into nine main macrocomponents having uniform elastic characteristics. These are the marlstone and clay soil components, the basement with foundation, the buttresses, the drum, the dome, the lantern, the bell towers, and the tie-bars.

The average dimension of the mesh is about 0.8 m and varies from the lantern to the soil, which is fully restrained at its edges. Spring elements are used to model the slight interaction with adjacent structures, while link elements are used to model the reaction frames of the tie-bars, which in turn are modeled with beam elements. Figure 8 reports the FEM of the structure with macrocomponents highlighted in different shades of gray, and the nominal values of the mechanical parameters used in the analyses.

Starting from the FEM, it was then necessary to ensure that the model was also able to reproduce the trend observed for the natural frequencies as a function of temperature, in order to generate the SD training data set. Furthermore, in order to simulate the uncertainty obtained from experimental estimates at constant temperature, that is, variation of the mechanical parameters due to in-field observation (e.g., EOVs other than temperature, instrumentation errors), a Gaussian distribution was used to generate noise samples to add to the previously mentioned modulus–temperature law.

Since a simple sensitivity analysis on the FE model highlighted that the variation of the first three natural frequencies is mainly influenced by the basement and foundation system, in the analyses, only the Young's modulus of this masonry macrocomponent was sampled to generate the SD. To this aim, a Gaussian noise of 10% was applied to the value of the modulus, in line with literature (Saloustros et al., 2019) and considering the variability of the results of the available experimental tests (Aoki et al., 2011). For each temperature level, it was thus possible to sample different values of Young's modulus. In particular, a total of 100 eigenvalue problems (i.e., 50 relating to a temperature of 10°C and 50 to a temperature of 3°C) were solved using FE analysis, where the equivalent Young's modulus of the basement and foundation was changed in accordance with the assumed modulus–temperature law.

The Young's modulus–temperature law adopted for this application depends on the thermal expansion coefficient of water (for further information and physical interpretations the reader can refer to Coletta et al., 2021) and reads:

$$E(T) \approx E_0 \left[1 + \alpha_{\mathrm{H2O}}(T)\, T\right] \tag{7}$$

where T is the absolute temperature, $E(T)$ the Young's modulus, $\alpha_{\mathrm{H2O}}(T)$ the coefficient of thermal expansion of water, and E_0 a parameter of the law obtained by fitting the experimental temperature–natural frequency law of the first two modes of the Sanctuary. $\alpha_{\mathrm{H2O}}(T)$ was obtained by fitting the data reported in https://webbook.nist.gov/chemistry/ about the density of water ρ at different temperatures (Moore & Molinero, 2011; Tanaka, 1998), with a

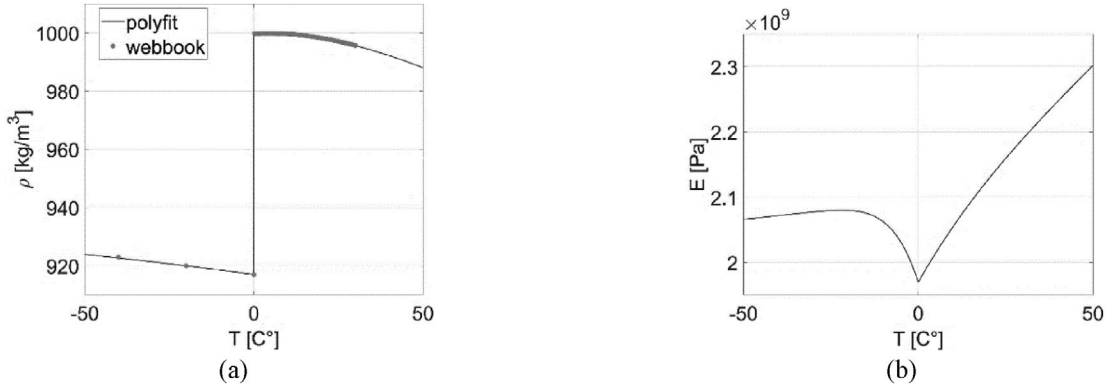

FIGURE 9 Density ρ of water (a); and the related temperature-equivalent Young's modulus law (b).

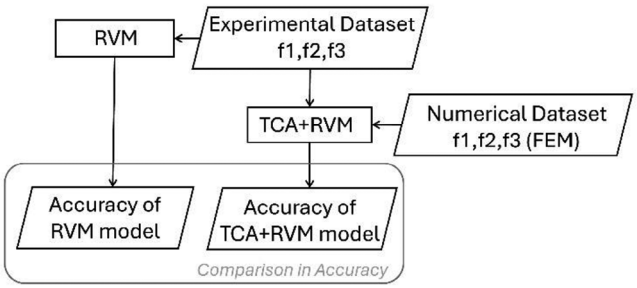

FIGURE 10 Flow chart to verify the first branch of the proposed methodology in the case of the Sanctuary of Vicoforte.

TABLE 1 Summary of the accuracies reached with the two models during the test phase (global and single classes).

Model (machine learning [ML] transfer learning [TL])	Global accuracy	Single class accuracy	
		Class 1	Class 2
Relevance vector machine (RVM)	62.8%	70.6%	60.9%
Transfer component analysis (TCA) + RVM	79.1%	76.5%	79.7%
Δacc	16.3%	5.9%	18.8%

12-order polynomial law, using Equation (7):

$$\alpha_{H2O}(T) = -\frac{1}{\rho(T)}\frac{\partial \rho(T)}{\partial T} \tag{8}$$

Figure 9 reports the density of water as function of temperature, and the assumed temperature-equivalent Young's modulus law. The estimate of modal frequencies deriving from this model had already been confirmed to be fully compliant with the experimental results in terms of the trend of modal frequencies as a function of temperature (Coletta et al., 2021; Pecorelli et al., 2020).

A comparison is always necessary between a simple ML, trained on one domain that considers data from monitoring activities and FEM together, and a TL methodology that considers the two data sets as different domains, see Figure 10. This is done because the SD shows some differences compared to the TD (Figure 11a), as in the first case, the two classes do not present an overlapping region and the two point clouds are less scattered. In fact, if the results obtained from the two models were almost the same, it would no longer make sense to use TL algorithms.

In line with the above, an RVM classifier was first deduced on the data of the Sanctuary of Vicoforte, without considering the differences between the monitored data set and the simulated data set. For the kernel representation of the data set a radial basis function (RBF) has been chosen, for which the kernel scale parameter σ has been fixed as the value for which the maximum average classification accuracy of a *fivefold cross-validation* procedure has been reached ($\sigma = .3$). The model has been trained on 15 observations of class 1 and no observations of class 2 for the TD, and on all the points of the SD. Then, it was tested on the remaining points (Figure 11c).

Second, a DA technique has been used to reduce the distance between the data distribution of the two domains, before generating a pattern with an RVM algorithm. In this case, a quadratic kernel has been used, and a *fivefold cross-validation* procedure was performed, thus the hyperparameters, which returned the highest average accuracy, were selected. The adaptation procedure results in a number of transfer component equal to 2, a regularization parameter $\mu = 10^{-7}$ and a kernel scale equal to 15, while for the classification, a Gaussian kernel has been selected with $\sigma = 2.9$. The parameters μ and σ are dimensionless.

The original data set has been dimensionally reduced and projected into a bidimensional latent subspace (z_1, z_2), which does not have a physical meaning, but is a mathematical expedient that tries to bring the domains as close as possible (Figure 11b). This second model has been trained and tested on the same data used for the previous classifier (Figure 11d). An overview of the accuracies achieved by the two models is presented in Table 1, together with the accuracy achieved for each individual class. For the RVM model, without prior DA, an accuracy of 62.8% is

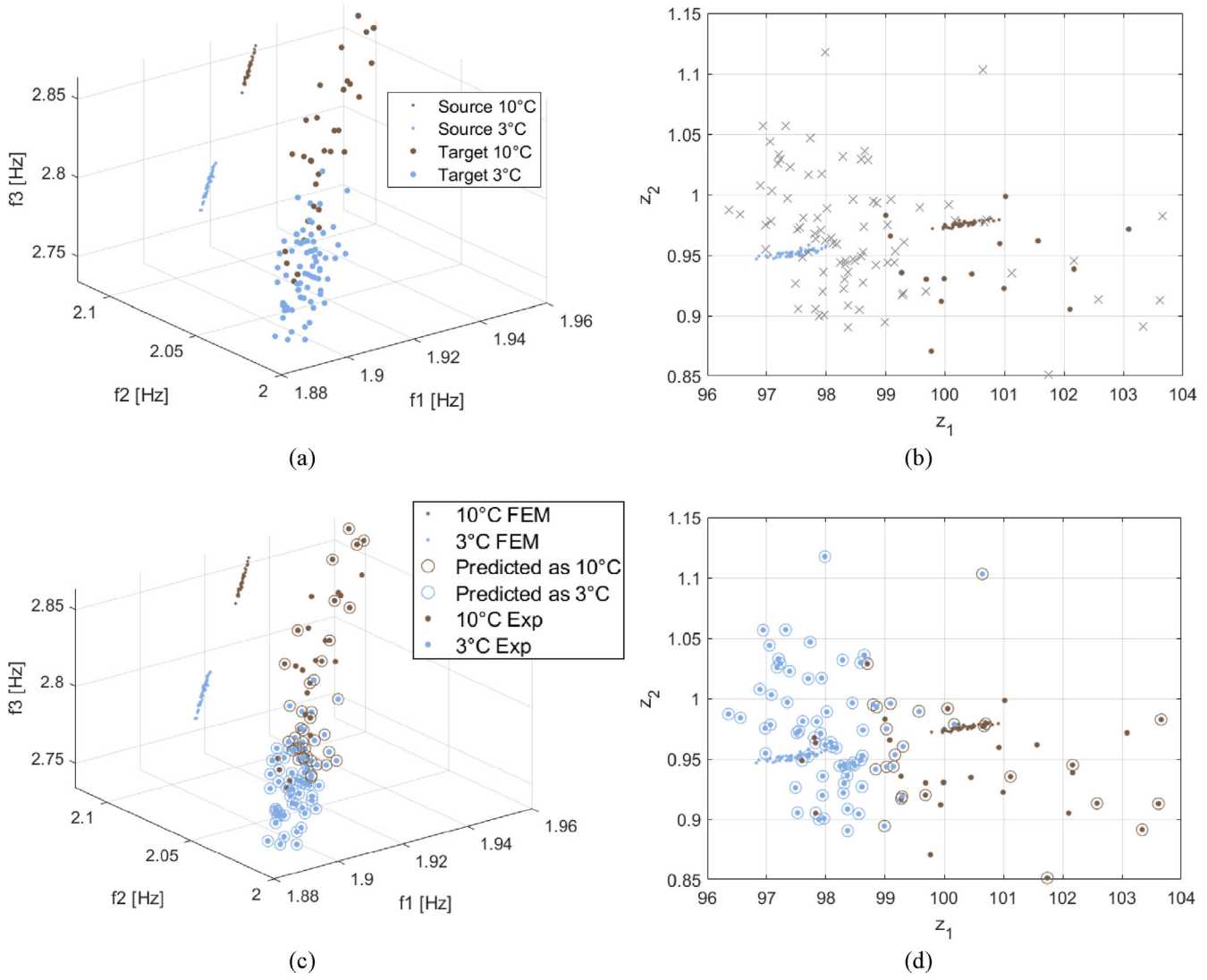

FIGURE 11 (a) Target and source domain; (b) projection of the domains in the latent subspace representation (z_1, z_2) obtained through transfer component analysis (TCA); (c) relevance vector machine (RVM) model inferred without preliminary domain adaptation; and (d) RVM model inferred in the latent subspace representation (z_1, z_2). The models are trained on the not circled data and tested on the remaining ones, the circles color represent the model prediction.

reached; while for the RVM model inferred after the DA, an accuracy of 79.1% is reached. Hence, the application of TCA upstream of the definition of the classification model with the RVM algorithm resulted in an increase in prediction accuracy of 16.3%. This means that the FEM of the Sanctuary does not perfectly adhere to the real structure, therefore it is better not to *mix* the monitoring system data with the model data and perform a DA each time to reduce the distance between the data distribution.

4.2 | TL from an experimental data set to another experimental data set

TL can be used to enrich experimental data sets of structures deemed insufficiently monitored to cover all possible structural conditions. In this section, the SD is used as the one that contains data coming from similar existing structures, but which are monitored exhaustively, or in any case with more data available. To demonstrate this approach, the experimental monitoring data of the Sanctuary of Vicoforte (*SD*) are exploited to expand the data set necessary for a linear classifier to predict temperature states of the Church of Santa Caterina (*TD*). In addition, to obtain a basis of comparison for performance evaluation of the DA procedure also a simple ML, namely support vector machine (SVM), trained only on the TD is developed (see Figure 12).

For this purpose, only a subset of the data actually available from the Santa Caterina monitoring is used, so that it can be considered insufficient for classification, but so that there is enough data left for testing

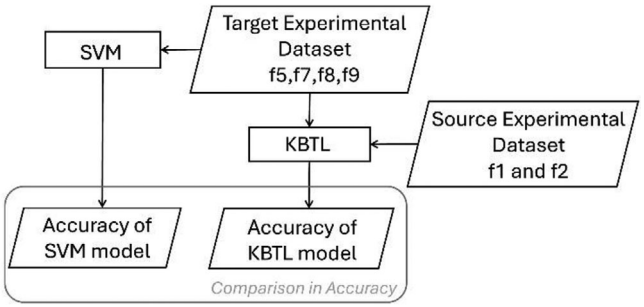

FIGURE 12 Flow chart to verify the second branch of the proposed methodology for the Church of Santa Caterina (target) and Sanctuary of Vicoforte (source).

the generated classification models (SVM and KBTL model).

Referring to the Church of Santa Caterina, all the natural frequencies detectable in Figure 5c and d were considered, except for local modes (e.g., mode 6 that is ruled by the façade) and high-frequency modes 10 and 11, that are typically noisy. Figure 13a–d reports the modal shapes associated to the selected vibration frequencies. Among the frequency-temperature laws of these four modes considered, only those values identified at temperatures in ranges [1.5°C, 3.5°C], [8.5°C, 9.5°C] and [15°C, 18°C] are selected for the TL model definition (i.e., three classes/labels are defined, *class 1*, *class 2* and *class 3*, respectively). Consequently, from the monitoring activities of December 2022 to March 2023 are available 112 observations for class 1, 157 observations for class 2, and 32 observations for class 3, for a total of 301 observations. For the training of the algorithms (SVM and KBTL) only 18 observations, randomly drawn, for each class are used, while the remaining 247 observations are considered as test data set (Figure 14a).

Additionally, for the training of the KBTL model also data of the Sanctuary of Vicoforte (*SD*) are exploited, specifically the first two natural frequencies f_1 and f_2 (i.e., translation modes along the dome minor and major axis). Figure 13e,f reports the mode shapes associated to the two vibration frequencies selected for the Sanctuary. The authors' choice to consider only two of the seven natural frequencies of the Sanctuary is dictated by various reasons. First, modes 4 to 7 are excluded because they mostly involve the same structural elements as the two translation ones, and therefore contain little useful information for the classifier. Mode 3 was also excluded, as it is a torsional mode, which is underrepresented in the dynamic response of the Church of Santa Caterina and therefore f_3 would be unhelpful for the classification of its data. Furthermore, unlike the first two frequencies, for this third frequency much fewer observations are available and therefore, to avoid a substantial reduction of the Vicoforte data set, it was not considered. The source data set is composed by

TABLE 2 Observations for each class for the training and test of the SVM and kernelized Bayesian transfer learning (KBTL) model for the classification of the insufficiently monitored system data (Church of Santa Caterina).

Model	Church	Class	Training	Test
SVM	Church of Santa Caterina	y = 1	18	94
		y = 2	18	139
		y = 3	18	14
	Sanctuary of Vicoforte	y = 1	0	0
		y = 2	0	0
		y = 3	0	0
KBTL	Church of Santa Caterina	y = 1	18	94
		y = 2	18	139
		y = 3	18	14
	Sanctuary of Vicoforte	y = 1	100	0
		y = 2	100	0
		y = 3	100	0

the same three temperature classes of the TD, specifically 100 observations for each classes (Figure 14b). In Table 2, a summary of the domains and the number of observations used to train and test the models is presented.

First, an ML model is generated from data of only the Church of Santa Caterina to understand and verify whether it is possible to generate, from a small amount of data, a predictive model that does not overfit the data provided in training and thus generalizes well for unseen data. To solve this classification problem, the choice fell on a linear classifier, that is, an SVM (Salcedo-Sanz et al., 2014), in consideration of the possible causes that may generate an overfitting problem. Indeed, overfitting is generally attributable to two main causes, either too small size of the training data set and/or too high degree of the classifier polynomial (Ying, 2019). As a result of this, having only 54 observations (18 for each class) available to train the model, a linear classifier avoids the introduction of an additional factor, along with the limitations of the data set, that may induce overfitting. In a nutshell, an SVM model attempts to maximally separate data by hyperplanes (linear law), finding a low-density region between classes. To easily separate the data with a linear law, the kernel representation is generally applied to transfer the initial data set into a larger, possibly infinite size space, that is, the RKHS (Salcedo-Sanz et al., 2014). To find the optimal solution the *Classification Learner MATLAB Toolbox* was used, specifically the *optimizable SVM*, which led to a one-versus-one classifier and using a linear kernel function with scaling parameter set equal to 1 in order to manipulate the input data set. The model obtained is shown in Figure 15a, where the correct labels are presented with the color of the dots, while the predictions are highlighted by the color of the

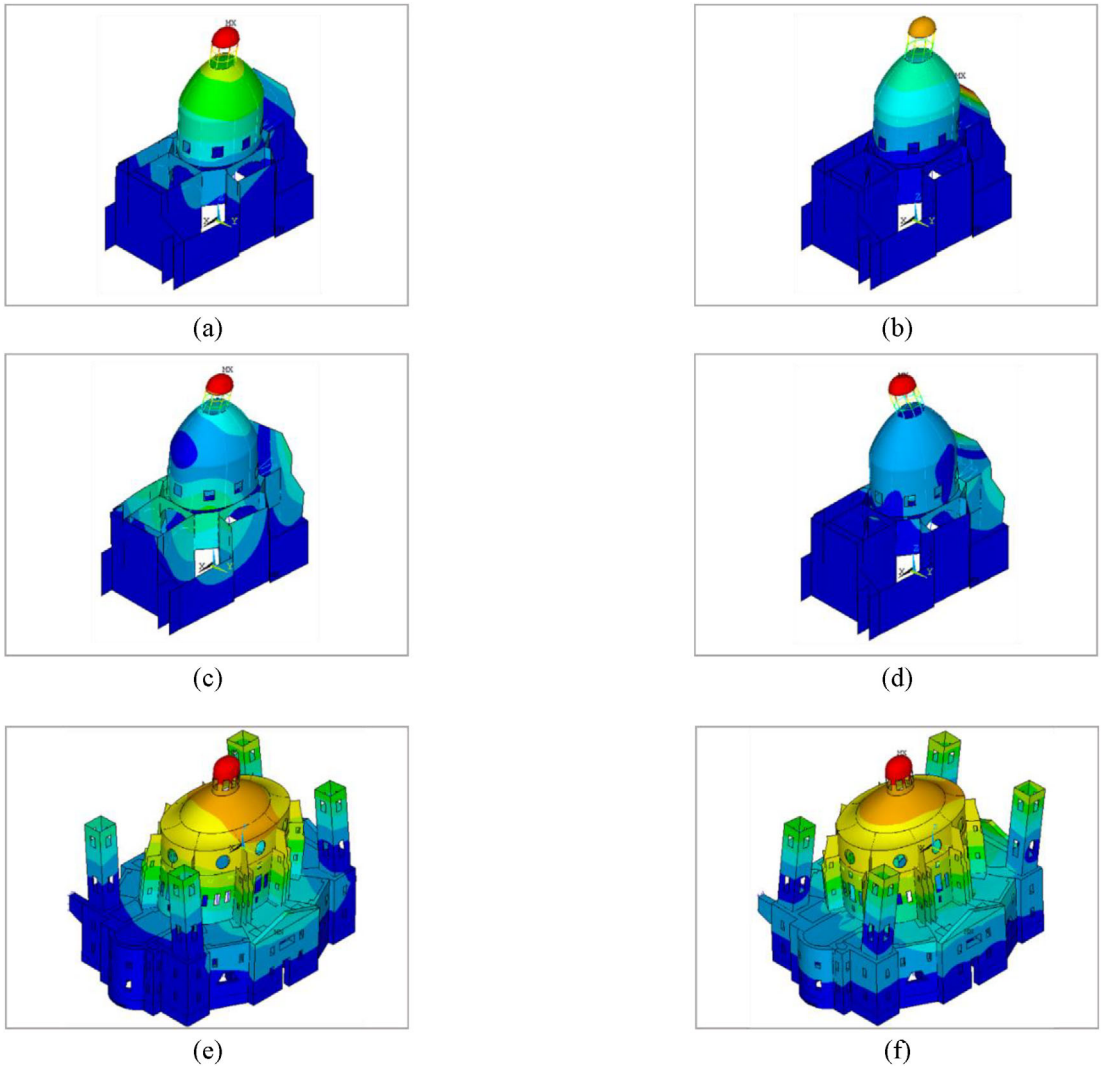

FIGURE 13 Mode shapes of the two churches for the selected features of target and source domains. Church of Santa Caterina: (a) Mode 5, (b) Mode 7, (c) Mode 8, and (d) Mode 9; Sanctuary of Vicoforte: (e) Mode 1 and (f) Mode 2.

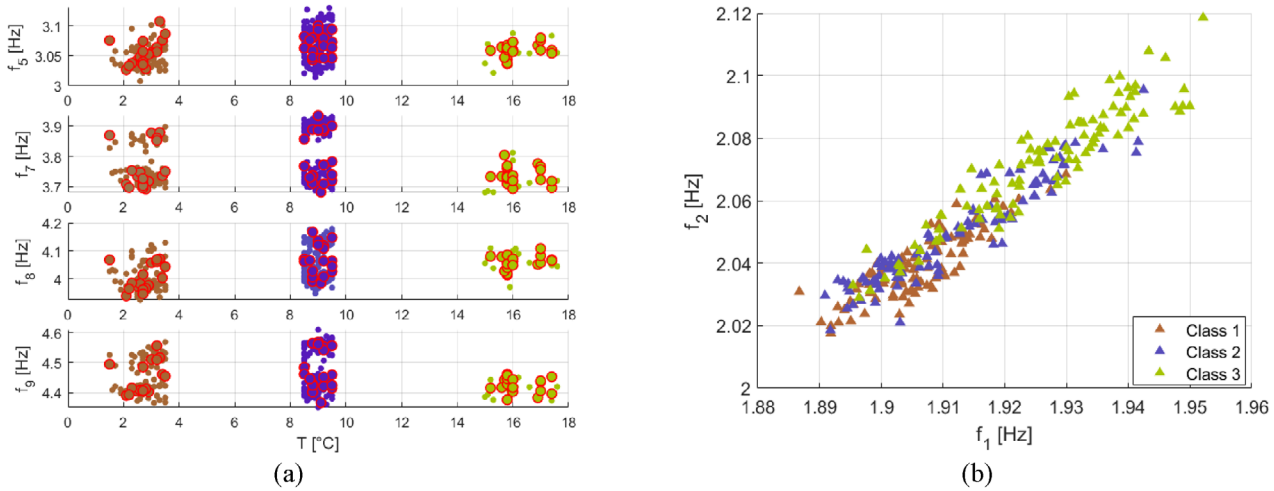

FIGURE 14 (a) Training and test domain of the Church of Santa Caterina. The test data set is composed by data circled in red, the remaining data are the training data set; and (b) source domain (Sanctuary of Vicoforte) for the training of the kernelized Bayesian transfer learning (KBTL) model.

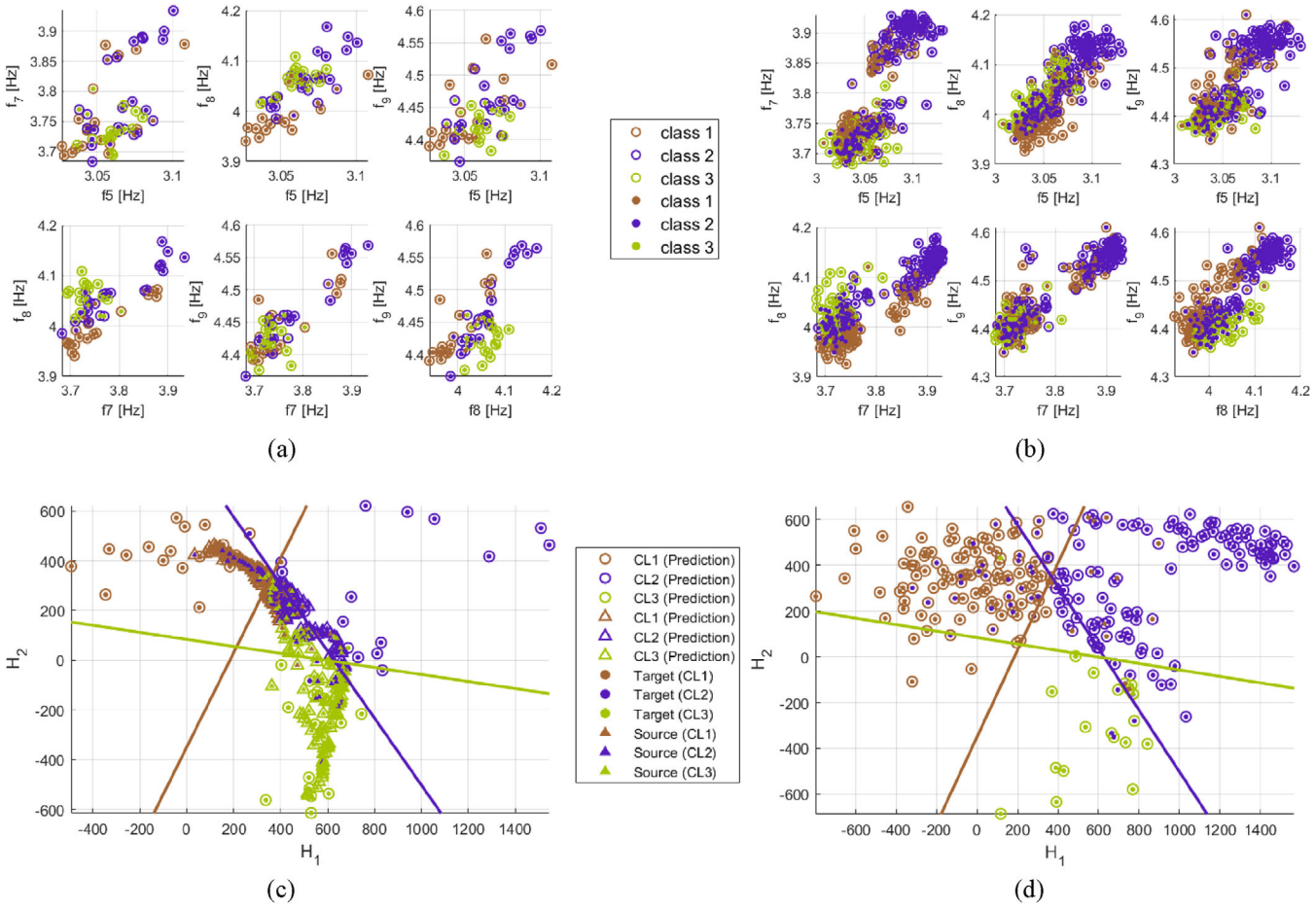

FIGURE 15 (a) SVM model obtained providing a training data set consisting of only 54 observations obtained for Church of Santa Caterina (projections of the four-dimensional space); (b) testing of SVM model; (c) training phase of kernelized Bayesian transfer learning (KBTL) model, trained on 54 observations of the Church of Santa Caterina (circle) and on 300 observations of the Sanctuary of Vicoforte (triangle); and (d) testing of the KBTL model.

circles around the dots. In this training phase, according to *fivefold cross-validation*, an accuracy of 75.93% is reached. Subsequently, the remaining 247 observations from the monitoring of the Church of Santa Caterina are used to test the model generated above, whose results are shown in Figure 15b. In this test phase, a global accuracy of 69.64% is reached by the model.

As a result of the testing phase, the accuracy of the SVM model is approximately of only 69% and for this reason an alternative approach involving a DA procedure is justifiable to enhance predictive capability. This is accomplished with the support of the KBTL algorithm, a specific TL technique based on DA, which allows knowledge to be shared from the exhaustively monitored dome, the Sanctuary of Vicoforte, to the Church of Santa Caterina. For simplicity, going forward, the Sanctuary of Vicoforte and the Church of Santa Caterina will be designed as SD and TD, respectively.

To train the algorithm, 54 observations for the TD and 300 observations for the SD are considered. As it is evident from Section 2.2, the KBTL model is generated using an extensive set of hyperparameters that requires careful handling. These hyperparameters were initially set based on the authors' expectation and on the input parameters analysis. Subsequently, they were slight modified until the model achieved the highest accuracy without visible overfitting, that is, manual tuning. At the end of this process, the following values were selected: a latent subspace dimension $\mathcal{R}$ equal to 2, a number of iteration equal to 1000, the priors hyperparameters $\alpha_\lambda, \beta_\lambda, \alpha_\gamma, \beta_\gamma, \alpha_\eta, \beta_\eta$ equal to .076, a latent subspace variance σ_h^2 equal to 9 and a nonnegative margin ν equal to 1. A brief explanation of the reasons behind these choices follows. First of all, the latent subspace dimension equal to 2 permits the model representation for visual checks of any overfitting problems, while the number of iterations fixed to 1000 is sufficiently high while still involving a reasonable computation time. The prior hyperparameters were set equal to .076, following a process in which they were made to vary within the limited range [.001, .1]. The boundaries

of this range were established based on two considerations. First, because of the hierarchical nature of the KBTL, the posterior distribution should exhibit limited sensitivity to the prior hyperparameter choices. Second, due to the small sample size, the two hyperparameters for each prior should be small values (Gardner et al., 2022). The latent subspace variance σ_h^2 is set equal to 3^2, as a rather large value is needed (several attempts were developed varying this parameter between 1^2 and 7^2), to reflect the expectation of finding a latent subspace in which the two domains are quite sparse, as there are notable differences between the dynamic responses of the two structures considered. Finally, the nonnegative margin ν is set equal 1 to force the algorithm to find in the latent subspace a margin among classes with a small data density. For the kernel representation (Herbrich, 2001), both the linear function and the RBF were analyzed. However, the final model was obtained with the RBF, where the handling of the weight hyperparameters γ_k (one for each training domain) was solved with a *median heuristics* approach, proposed by Gretton et al. (2012) and successfully applied in the SHM field by Gardner et al. (2022). The RBF takes as input the matrix of the observed features of the kth domain, $\mathbf{X}_k$, and represents it with its kernel matrix, $\mathbf{K}_k$. The RBF kernel is defined as $k_k(\mathbf{x}, \mathbf{x}') = \exp(-\gamma_k \|\mathbf{x} - \mathbf{x}'\|^2)$, with $\|\mathbf{x} - \mathbf{x}'\|^2$ the squared Euclidean distance.

The model generated during the training phase of the KBTL is shown in Figure 15c, where the TD is presented with the dot-circle system while the SD with filled triangle-empty triangle system. The dots and the filled triangles define with their colors the label to be predicted by the algorithm, while the circles and the empty triangles show with their colors the label predicted by the algorithm for that given data. The training accuracy achieved by this model in predicting the temperature states of the TD is 87.04%.

Subsequently, the model generated above was tested for the remaining 247 observations retrieved from the monitoring activities developed on the target structure. In Figure 15d, the KBTL model is applied to predict the target unseen data. The figure is composed like the training one, with the difference that only data belonging to the TD are present (dot-circle). For this test phase, the model led to an overall accuracy in predicting the TD temperature states of 80.57%.

Finally, in Table 3, a summary of the accuracy reached by the two classification models—SVM and KBTL—is proposed to demonstrate the applicability and the efficiency of the proposed methodology for the two churches. Specifically, the accuracy reached during the training phase and test phase of the two algorithms is reported, highlighting the test accuracy achieved in the predictions of each single class. The transition from the SVM model, trained only using data from the Church of Santa Caterina, to the KBTL model, trained also on data from the Sanctuary of Vicoforte, led to an increment in the predictive accuracy of ∼11% for the Church of Santa Caterina. Since a homogeneous data set was not provided during the test phase, it was necessary to analyze the accuracy with which each individual class was predicted. From this analysis, a further demonstration of the effectiveness of the DA can be obtained. In fact, by comparing the accuracy achieved by each class before and after the application of the DA, a percent increase in the range $6\% - 14\%$ was observed.

TABLE 3 Comparison between the accuracies reached by the two applied model, SVM and kernelized Bayesian transfer learning (KBTL), during the training phase and test phase. With the explication of the accuracies reached in the prediction of each class during the test phase.

Phase	Accuracy SVM	Accuracy KBTL	Variation
Training	75.93%	87.04%	+11.11%
Test	69.64%	80.57%	+10.93%
Class 1 - test	80.85%	87.23%	+6.38%
Class 2 - test	61.15%	74.82%	+13.67%
Class 3 - test	78.57%	92.86%	+14.29%

Ultimately, the use of data from the Sanctuary of Vicoforte, through DA, proved to be beneficial in generating a predictive model for the Church of Santa Caterina. Indeed, even if limited data for the TD were available for the training phase of the classifier, the final test accuracy exceeded 80%.

5 | CONCLUSIONS

In this paper, different TL approaches, based on DA, have been investigated in order to define a methodology for assessing the structural condition states in monitored historical domes. The methodology was designed to allow diagnostic evaluations even on very complex structures for which limited and incomplete monitoring data are available, by transferring knowledge between different monitoring systems and models.

Specifically, two different TL applications have been proposed. The first revealed how the implementation of a homogeneous DA strategy can exploit additional information retrievable from a mathematical model, in order to implement the recognition of different temperature states from monitoring data. The second demonstrated how a monitoring program very rich in information can contribute to improving knowledge of a structure with a

certain similarity but with a less complete monitoring data, thorough heterogeneous DA. The proposed methodology was applied to two churches, namely the Sanctuary of Vicoforte and the Church of Santa Caterina, in order to demonstrate its effectiveness. Overall, a reduction in accuracy from training to testing was found in the analyses. This might be explained in two ways: an overfitting case or, more likely, an effect of the different amount of data used in the training and testing phases, to simulate a real data availability condition. At any rate, the results can be summarized as follows:

1. The first application type was solved by adapting the domains through TCA and classifying data with an RVM model, which led to an enhancement of the testing prediction accuracy of 16.3%, compared with the unadapted case.
2. The second application type was implemented via the KBTL algorithm, which led to an improvement of the testing prediction accuracy of 10.93% compared to an SVM model.

The results obtained in these presented studies constitute proofs of strength, which are believed to encourage a systematic application of DA in the field of monitoring complex full-scale structures. Historical and monumental structures, in addition to being geometrically and mechanically complex, have the characteristic of uniqueness. Precisely for this reason, it is not easy to develop an experience in terms of symptoms and thresholds that can be exploited directly for diagnostic purposes. Transferring knowledge between experimental data sets, also thanks to the new potential offered by AI, would be even more strategic in this sector. Conversely, rigorous criteria are needed to identify classes of structures that can be considered similar from the TL point of view.

In future developments, this methodology may be used for the classification of more general structural conditions (e.g., damaged ones), for which very few observations are available. This will be done by exploiting numerical and experimental datasets from other structures, but also by undertaking a comprehensive process to select the most suitable DA algorithm to refine the methodology. To this end, a systematic performance comparison between various available TL methods will be carried out.

ACKNOWLEDGMENTS

The authors gratefully acknowledge the Santa Caterina Onlus, the Amministrazione del Santuario di Vicoforte, and the Fondazione CRC. This study was carried out within the «SAT4SHM » project—funded by European Union—Next Generation EU within the PRIN 2022 PNRR program (D.D.1409, 14/09/2022 MIUR).

Open access publishing facilitated by Politecnico di Torino, as part of the Wiley - CRUI-CARE agreement.

REFERENCES

Adeli, H., & Hung, S.-L. (1994). *Machine learning: Neural networks, genetic algorithms, and fuzzy systems*. John Wiley & Sons, Inc.

Amezquita-Sancheza, J., Valtierra-Rodriguez, M., & Adeli, H. (2020). Machine learning in structural engineering. *Scientia Iranica*, *27*(6), 2645–2656.

Aoki, T., Yuasa, N., Hamasaki, H., Nakano, Y., Takahashi, N., Tanigawa, Y., Komiyama, T., Ina, T., Sabia, D., & Demarie, G. V. (2011). Safety assessment of the Sanctuary of Vicoforte, Italy. *International Journal of Materials and Structural Integrity*, *5*(2–3), 215–240.

Boscato, G., Russo, S., Ceravolo, R., & Fragonara, L. Z. (2015). Global sensitivity-based model updating for heritage structures. *Computer-Aided Civil and Infrastructure Engineering*, *30*(8), 620–635. https://doi.org/10.1111/mice.12138

Bull, L. A., Gardner, P. A., Gosliga, J., Dervilis, N., Papatheou, E., Maguire, A. E., Campos, C., Rogers, T. J., Cross, E. J., & Worden, K. (2020). Towards population-based structural health monitoring, Part I: Homogeneous populations and forms. In Z. Mao (Ed.), *Model validation and uncertainty quantification* (Vol. 3, pp. 287–302). Springer International Publishing.

Bursi, O. S., Kumar, A., Abbiati, G., & Ceravolo, R. (2014). Identification, model updating, and validation of a steel twin deck curved cable-stayed footbridge. *Computer-Aided Civil and Infrastructure Engineering*, *29*(9), 703–722. https://doi.org/10.1111/mice.12076

Ceravolo, R., Coletta, G., Miraglia, G., & Palma, F. (2021). Statistical correlation between environmental time series and data from long-term monitoring of buildings. *Mechanical Systems and Signal Processing*, *152*, 107460. https://doi.org/10.1016/j.ymssp.2020.107460

Ceravolo, R., De Lucia, G., Miraglia, G., & Pecorelli, M. L. (2020). Thermoelastic finite element model updating with application to monumental buildings. *Computer-Aided Civil and Infrastructure Engineering*, *35*(6), 628–642. https://doi.org/10.1111/mice.12516

Ceravolo, R., De Marinis, A., Pecorelli, M. L., & Zanotti Fragonara, L. (2017). Monitoring of masonry historical constructions: 10 years of static monitoring of the world's largest oval dome. *Structural Control and Health Monitoring*, *24*(10), e1988. https://doi.org/10.1002/stc.1988

Ceravolo, R., Lenticchia, E., Miraglia, G., & Scussolini, L. (2024). Improving the dynamic behaviour of historic buildings using experimental data: Application to a Baroque church. *Journal of Civil Structural Health Monitoring*, 1–20. https://doi.org/10.1007/s13349-024-00804-x

Ceravolo, R., Pistone, G., Fragonara, L. Z., Massetto, S., & Abbiati, G. (2016). Vibration-based monitoring and diagnosis of cultural heritage: A methodological discussion in three examples. *International Journal of Architectural Heritage*, *10*(4), 375–395. https://doi.org/10.1080/15583058.2013.850554

Chakraborty, D., Kovvali, N., Chakraborty, B., Papandreou-Suppappola, A., & Chattopadhyay, A. (2011). Structural damage detection with insufficient data using transfer learning techniques. In *Sensors and Smart Structures Technologies for Civil, Mechanical, and Aerospace Systems* (Vol. 7981, pp. 1175-1183). Proceedings of the SPIE. https://doi.org/10.1117/12.882025

Coletta, G., Miraglia, G., Gardner, P., Ceravolo, R., Surace, C., & Worden, K. (2021). A transfer learning application to FEM and monitoring data for supporting the classification of structural condition states. In P. Rizzo & A. Milazzo (Eds.), *European workshop on structural health monitoring: Special collection of 2020 papers* (Vol. 1, pp. 947–957). Springer International Publishing. https://doi.org/10.1007/978-3-030-64594-6_91

Farahani, A., Pourshojae, B., Rasheed, K., & Arabnia, H. R. (2020). A concise review of transfer learning. In *2020 international conference on computational science and computational intelligence (CSCI)* (pp. 344–351). IEEE. https://doi.org/10.1109/CSCI51800.2020.00065

Farrar, C. R., & Worden, K. (2012). *Structural health monitoring: A machine learning perspective*. John Wiley & Sons.

Friswell, M., & Mottershead, J. E. (1995). *Finite element model updating in structural dynamics* (Vol. 38). Springer Science & Business Media.

Gao, Y., & Mosalam, K. M. (2018). Deep transfer learning for image-based structural damage recognition. *Computer-Aided Civil and Infrastructure Engineering*, *33*(9), 748–768. https://doi.org/10.1111/mice.12363

Gardner, P., Bull, L. A., Dervilis, N., & Worden, K. (2022). On the application of kernelised Bayesian transfer learning to population-based structural health monitoring. *Mechanical Systems and Signal Processing*, *167*, 108519. https://doi.org/10.1016/j.ymssp.2021.108519

Gardner, P., Bull, L. A., Gosliga, J., Dervilis, N., & Worden, K. (2020). Towards population-based structural health monitoring, Part IV: Heterogeneous populations, transfer and mapping. In Z. Mao (Ed.), *Model validation and uncertainty quantification* (Vol. 3, pp. 187–199). Springer International Publishing.

Gardner, P., Liu, X., & Worden, K. (2020). On the application of domain adaptation in structural health monitoring. *Mechanical Systems and Signal Processing*, *138*, 106550. https://doi.org/10.1016/j.ymssp.2019.106550

Garro, M. (1962). The Sanctuary of Vicoforte: Strengthening and rehabilitation works (in Italian). Technical report. Historical Archive of the Sanctuary of Vicoforte (Cuneo), Italy.

Giglioni, V., Poole, J., Venanzi, I., Ubertini, F., & Worden, K. (2024). A domain adaptation approach to damage classification with an application to bridge monitoring. *Mechanical Systems and Signal Processing*, *209*, 111135. https://doi.org/10.1016/j.ymssp.2024.111135

Gönen, M., & Margolin, A. (2014). Kernelized Bayesian transfer learning. *Proceedings of the AAAI Conference on Artificial Intelligence*, *28*(1), 1831–1839. https://doi.org/10.1609/aaai.v28i1.8948

Gretton, A., Sejdinovic, D., Strathmann, H., Balakrishnan, S., Pontil, M., Fukumizu, K., & Sriperumbudur, B. K. (2012). Optimal kernel choice for large-scale two-sample tests. In F. Pereira, C. J. Burges, L. Bottou, & K. Q. Weinberger (Eds.), *Advances in neural information processing systems* (Vol. 25, pp. 1205–1213). Curran Associates, Inc. https://proceedings.neurips.cc/paper_files/paper/2012/file/dbe272bab69f8e13f14b405e038deb64-Paper.pdf

Herbrich, R. (2001). *Learning kernel classifiers: Theory and algorithms*. MIT Press.

Huang, Q., Wang, J., Song, Y., Cui, W., Li, H., Wang, S., Dai, P., Zhao, X., & Li, Q. (2024). Synthetic-to-realistic domain adaptation for cold-start of rail inspection systems. *Computer-Aided Civil and Infrastructure Engineering*, *39*(3), 424–437. https://doi.org/10.1111/mice.13087

Javadinasab Hormozabad, S., Gutierrez Soto, M., & Adeli, H. (2021). Integrating structural control, health monitoring, and energy harvesting for smart cities. *Expert Systems*, *38*(8), e12845. https://doi.org/10.1111/exsy.12845

Li, Y., Che, P., Liu, C., Wu, D., & Du, Y. (2021). Cross-scene pavement distress detection by a novel transfer learning framework. *Computer-Aided Civil and Infrastructure Engineering*, *36*(11), 1398–1415. https://doi.org/10.1111/mice.12674

Lin, Y., Nie, Z., & Ma, H. (2022). Dynamics-based cross-domain structural damage detection through deep transfer learning. *Computer-Aided Civil and Infrastructure Engineering*, *37*(1), 24–54. https://doi.org/10.1111/mice.12692

Moore, E. B., & Molinero, V. (2011). Structural transformation in supercooled water controls the crystallization rate of ice. *Nature*, *479*(7374), 506–508. https://doi.org/10.1038/nature10586

Pan, S. J., Tsang, I. W., Kwok, J. T., & Yang, Q. (2011). Domain adaptation via transfer component analysis. *IEEE Transactions on Neural Networks*, *22*(2), 199–210. https://doi.org/10.1109/TNN.2010.2091281

Pan, S. J., & Yang, Q. (2009). A survey on transfer learning. *IEEE Transactions on Knowledge and Data Engineering*, *20*(10), 1345–1359.

Pavlou, D. (2022). A deterministic algorithm for nonlinear, fatigue-based structural health monitoring. *Computer-Aided Civil and Infrastructure Engineering*, *37*(7), 809–831. https://doi.org/10.1111/mice.12783

Pecorelli, M. L., Ceravolo, R., & Epicoco, R. (2020). An automatic modal identification procedure for the permanent dynamic monitoring of the Sanctuary of Vicoforte. *International Journal of Architectural Heritage*, *14*(4), 630–644. https://doi.org/10.1080/15583058.2018.1554725

Perez-Ramirez, C. A., Amezquita-Sanchez, J. P., Adeli, H., Valtierra-Rodriguez, M., Camarena-Martinez, D., & Romero-Troncoso, R. J. (2016). New methodology for modal parameters identification of smart civil structures using ambient vibrations and synchrosqueezed wavelet transform. *Engineering Applications of Artificial Intelligence*, *48*, 1–12. https://doi.org/10.1016/j.engappai.2015.10.005

Perez-Ramirez, C. A., Amezquita-Sanchez, J. P., Valtierra-Rodriguez, M., Adeli, H., Dominguez-Gonzalez, A., & Romero-Troncoso, R. J. (2019). Recurrent neural network model with Bayesian training and mutual information for response prediction of large buildings. *Engineering Structures*, *178*, 603–615. https://doi.org/10.1016/j.engstruct.2018.10.065

Pezeshki, H., Adeli, H., Pavlou, D., & Siriwardane, S. C. (2023). State of the art in structural health monitoring of offshore and marine structures. *Proceedings of the Institution of Civil Engineers—Maritime Engineering*, *176*(2), 89–108. https://doi.org/10.1680/jmaen.2022.027

Pezeshki, H., Pavlou, D., Adeli, H., & Siriwardane, S. C. (2023). Modal analysis of offshore monopile wind turbine: An analytical solution. *Journal of Offshore Mechanics and Arctic Engineering*, *145*(1), 010907. https://doi.org/10.1115/1.4055402

Quqa, S., Landi, L., & Loh, K. J. (2023). Crack identification using electrical impedance tomography and transfer learning. *Computer-Aided Civil and Infrastructure Engineering*, *38*(17), 2426–2442. https://doi.org/10.1111/mice.13043

Rafiei, M. H., & Adeli, H. (2017). A novel machine learning-based algorithm to detect damage in high-rise building structures. *The*

Structural Design of Tall and Special Buildings, *26*(18), e1400. https://doi.org/10.1002/tal.1400

Salcedo-Sanz, S., Rojo-Álvarez, J. L., Martínez-Ramón, M., & Camps-Valls, G. (2014). Support vector machines in engineering: An overview. *WIREs Data Mining and Knowledge Discovery*, *4*(3), 234–267. https://doi.org/10.1002/widm.1125

Saloustros, S., Pelà, L., Contrafatto, F. R., Roca, P., & Petromichelakis, I. (2019). Analytical derivation of seismic fragility curves for historical masonry structures based on stochastic analysis of uncertain material parameters. *International Journal of Architectural Heritage*, *13*(7), 1142–1164.

Tanaka, H. (1998). Simple physical explanation of the unusual thermodynamic behavior of liquid water. *Physical Review Letters*, *80*(26), 5750–5753. https://doi.org/10.1103/PhysRevLett.80.5750

Tipping, M. E. (2001). Sparse Bayesian learning and the relevance vector machine. *Journal of Machine Learning Research*, *1*, 211–244.

Wang, X., & Xia, Y. (2022). Knowledge transfer for structural damage detection through re-weighted adversarial domain adaptation. *Mechanical Systems and Signal Processing*, *172*, 108991. https://doi.org/10.1016/j.ymssp.2022.108991

Ying, X. (2019). An overview of overfitting and its solutions. *Journal of Physics: Conference Series*, *1168*, 022022. https://doi.org/10.1088/1742-6596/1168/2/022022

How to cite this article: Cavanni, V., Ceravolo, R., & Miraglia, G. (2024). A domain adaptation methodology for enhancing the classification of structural condition states in continuously monitored historical domes. *Computer-Aided Civil and Infrastructure Engineering*, 1–20. https://doi.org/10.1111/mice.13313